

POLARIMETRY AT 1.3 mm USING MILLIPOL: METHODS AND PRELIMINARY RESULTS FOR ORION

RICHARD BARVAINIS^{a)}National Radio Astronomy Observatory,^{b)} Edgemont Road, Charlottesville, Virginia 22901DAN P. CLEMENS^{c)} AND ROBERT LEACH

Steward Observatory, University of Arizona, Tucson, Arizona 85721

Received 1 September 1987; revised 26 October 1987

ABSTRACT

We have constructed a polarimeter for use at wavelengths near 1 mm, designed to be self-contained and portable. Only minor modifications should be required to adapt this instrument for use on any of several millimeter and submillimeter telescopes. In this paper we describe the polarimeter system and data-taking techniques, and report a preliminary measurement of the polarized dust emission from the Orion KL region at 1.3 mm using the NRAO 12 m telescope. Our results ($P = 2.9 \pm 0.6\%$, $\chi = 11 \pm 6^\circ$) are similar to previous polarization measurements of Orion at far-infrared and submillimeter wavelengths. The magnetic field direction implied by the polarization position angle is parallel to that found in the surrounding Orion region using optical and near- to mid-infrared polarimetric techniques.

I. INTRODUCTION

The polarization of starlight by dust at optical and near-infrared wavelengths is due to selective absorption by non-spherical, spinning grains, which are aligned in magnetic fields. Observations of starlight polarization are routinely used to delineate field directions in the general interstellar medium and in the outer, low-density peripheries of molecular clouds. In some dense regions with warm imbedded infrared sources, near- and mid-infrared polarimetry can also be used to this end. However, in many potential or incipient sites of star formation, no polarized infrared sources are found, and the dust opacities in the optical/IR are so large that light from background stars cannot be detected; as a result, the magnetic field configurations in these regions are unknown. Attempts to map magnetic fields in dense clouds via linear polarization of molecular lines such as CO, first predicted theoretically by Goldreich and Kylafis (1981), have been unsuccessful (Wannier, Scoville, and Barvainis 1983; Barvainis and Wootten 1986).

While dust *absorption* obscures our view of dense cloud cores in the optical/IR, this same dust is optically thin at millimeter and submillimeter wavelengths and is strong in *emission* in many regions. Thus we might hope to use dust emission to decipher the structures of the densest parts of molecular clouds. It is known, via their polarization properties in absorption, that dust grains align with magnetic fields. We might also expect the emission from such grains to be polarized at optically thin millimeter/submillimeter wavelengths. That this is the case has been borne out by the work of Hildebrand, Dragovan, and Novak (1984, also reported in Dragovan 1986), who successfully measured linearly polarized dust emission at $270 \mu\text{m}$, using the *Kuiper Airborne Observatory* (KAO). They observed the Orion region with a $60''$ beam, and obtained a fractional polarization of about 1.7% at two different positions. Cudlip *et al.* (1982) also detected far-IR polarization in Orion at a wavelength of $77 \mu\text{m}$, with a $2'$ beam on a rocket-borne experiment. They mea-

sured a fractional polarization of 2.2% at a position angle similar to that of the $270 \mu\text{m}$ KAO observations.

Even though the spectrum of dust emission falls off rapidly toward longer wavelengths at submillimeter and millimeter wavelengths, a number of star-forming regions remain strong enough to be easily observed in total flux density at 1 mm using ground-based telescopes. Orion is the strongest, producing a peak flux density at 1.3 mm of nearly 100 Jy (in a $30''$ beam) at the KL position (Sutton *et al.* 1982; Gordon and Jewell 1987). Current telescope/receiver sensitivities are such that sources with tens of Janskys per beam should be amenable to polarimetric measurements at the 1%–2% level, with spatial resolutions a factor of 2 or more better than those available using the KAO at submillimeter wavelengths. With this in mind, we have built a polarimeter, MILLIPOL, for use at wavelengths near 1 mm. This device has been designed to be self-contained and fully portable, requiring only minor modifications for use at any of several existing millimeter telescope facilities (and at ground-based submillimeter telescopes in the future).

In this paper, we describe the MILLIPOL polarimeter, and discuss the methods of data collection and analysis used for its inaugural observing run at the NRAO 12 m telescope. We also present a preliminary report of the first detection of polarization at 1.3 mm (230 GHz), in the dust emission from the KL region of Orion. Although a detailed quantitative comparison of our results with those of Hildebrand, Dragovan, and Novak (1984, hereafter referred to as HDN) and Dragovan (1986) and Cudlip *et al.* (1982) is not possible because of the differences in beam sizes, we find that despite these differences and the differences in observing wavelengths our results for Orion are quite similar to the polarizations reported by those authors.

II. METHODS AND RESULTS

a) The Polarimeter System and Data-Taking Techniques

The MILLIPOL system (see Fig. 1) consists of (1) a rotating half-wave plate polarization analyzer which is mounted in the telescope beam path near the receiver feed, (2) a two-channel analog-to-digital converter, and (3) a Motorola VME 10 minicomputer for controlling the polarimeter and accumulating data. The half-wave plate is a

^{a)} Current address: Haystack Observatory, Westford, MA 01886.

^{b)} The National Radio Astronomy Observatory is operated by Associated Universities, Inc., under contract with the National Science Foundation.

^{c)} Bart J. Bok Fellow 1986–1987.

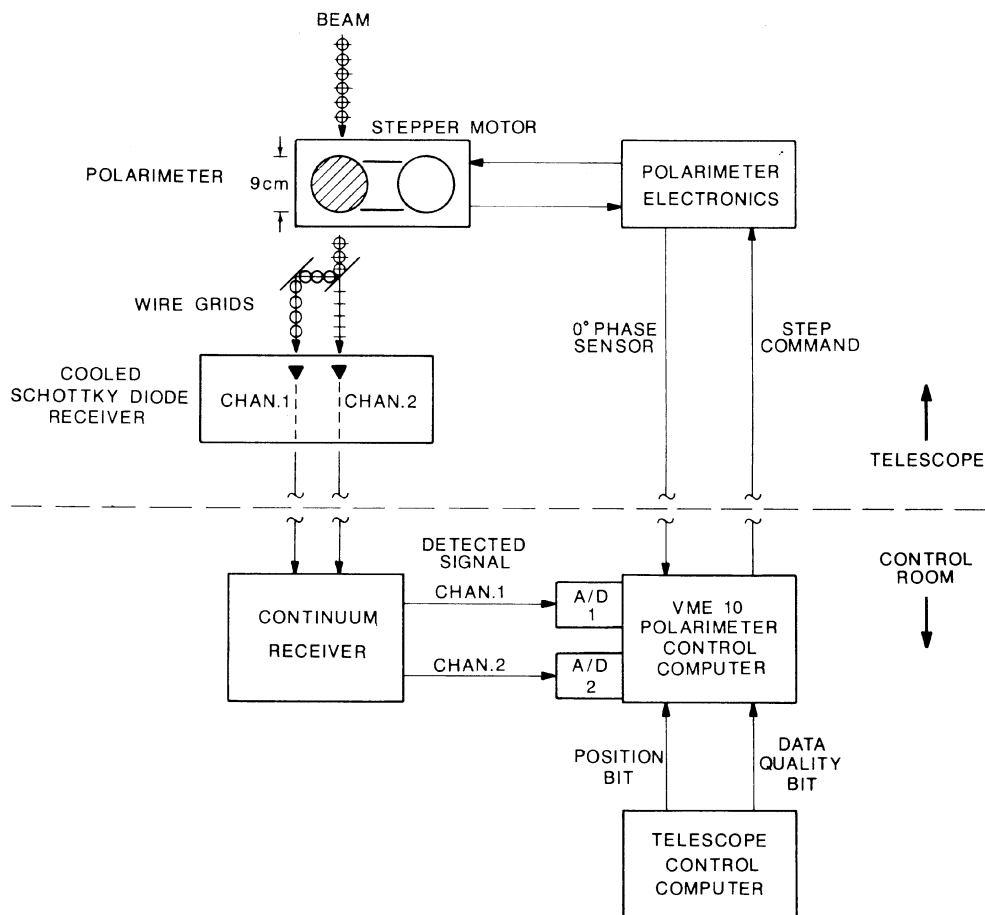


FIG. 1. Block diagram of relevant telescope and MILLIPOL system components, as configured on the NRAO 12 m telescope. The beam passes through the rotating polarization analyzer, and is then split into orthogonal polarizations, which are fed into the dual-channel cooled Schottky receiver. The detected analog signal is digitized using a two-channel A/D board and sampled by the polarimeter control computer. A stepper motor, commanded by the control computer, rotates the polarization analyzer via a plastic chain drive. A signal indicating the zero of polarimeter phase is returned to the control computer once each revolution. The polarimeter control computer continuously monitors position and data-quality bits passed from the telescope control computer, and stores or rejects data accordingly.

grooved dielectric type, fabricated from rexolite. This rotating plate, when used in conjunction with a linearly polarized feed, produces a modulation in the detected signal of the form

$$T(\theta) = \frac{1}{2} T_p \cos(4\theta - 2\phi), \quad (1)$$

where $T(\theta)$ is the modulated antenna temperature, T_p is the antenna temperature corresponding to the polarized flux density of the source, and the angle θ is the rotation angle of the plate. The phase ϕ is related to the position angle of the source polarization and the parallactic angle (since the 12 m telescope is altazimuth mounted):

$$\phi = \chi - \eta - \phi_{\text{offset}}, \quad (2)$$

where χ is the source position angle on the sky (measured eastward from north), η is the parallactic angle, and ϕ_{offset} is a constant phase offset (which must be calibrated). An additional sinusoidal modulation at 2θ , corresponding in amplitude to a few percent of the source total flux, arises because of the differential index of refraction of the plate for waves

polarized along the fast and slow axes (see Barvainis and Predmore 1984). Since this modulation is at a frequency different from that of the 4θ polarization signal, it can easily be removed from the data in postprocessing.

The rexolite plate is driven by a stepper motor with 1.8° increments, which is controlled by the minicomputer. The A/D converters are sampled at each step of the motor, digitizing the detected signals from the telescope's continuum backend. The MILLIPOL computer requires only two other bits of information from the host telescope: one bit specifying whether the telescope is pointed at the source position or the reference position, and one bit to specify data quality (telescope at the commanded coordinate position and receiver local-oscillator phase-lock loop in lock). Thus MILLIPOL can be used on any telescope where the polarimeter can be physically mounted in the beam (the aperture of the polarization analyzer is approximately 9 cm), where a detected continuum output is available, and where position and data-quality bits can be accessed.

To observe, the telescope need simply track the source and execute a standard position-switching sequence. The polar-

ization computer samples the A/Ds (at 320 Hz) and bins the data into 40 polarimeter angle bins, which are accumulated into source and reference buffers during the course of a scan. Typically, a scan consists of five 1 min source/reference pairs, with the polarimeter continuously rotating at a rate of 1.6 Hz. Although the polarization-switching rate is fairly high ($1.6 \times 4 = 6.4$ Hz, since the polarization is modulated at four times the rotation rate of the plate), information about the source total intensity is lost in polarization-switched observations of weak sources because the source/reference switching is too slow to cancel drifts in sky emission. Therefore, for weak sources (i.e., all except the Moon and planets) we must measure the total flux density separately using standard-continuum fast beam-switching techniques.

b) Observations, Analysis, and Calibration

The observations were made on 5–8 March 1987. The cooled, two-channel (orthogonal polarizations), Schottky diode receiver was optimized for double-sideband operation, with the upper sideband centered at 231.6 GHz and the lower sideband centered at 229.1 GHz. The observing frequency was chosen so as to minimize contributions from line radiation in the emission from Orion (Gordon and Jewell 1987). The effective bandwidth was 600 MHz. The beamwidth was measured to be $30''$, and pointing was monitored frequently using observations of the planets, which were also used to calibrate the flux-density scales. We estimate that the relative calibration between the total and polarized flux-density scales is accurate to approximately 10%. One receiver channel was found to be a factor of 2 noisier than the other, greatly limiting its usefulness for weak sources (for most of the results presented below, only the “good” channel is reported). All of the data reported here were obtained under excellent weather conditions.

A modest software package has been developed for displaying the data, calculating the power spectrum (to identify spurious periodic components), averaging scans, and extracting the source polarizations. We have found that the most favorable noise characteristics are generally obtained when the 40 polarization channels are folded, modulo the polarization period, to ten channels. This procedure effectively cancels the 2θ modulation mentioned above, and also significantly reduces most of the spurious Fourier components that occasionally appear in the data. Thus, the normal procedure is to fold the data into ten channels spanning a polarimeter-angle range of 0° – 90° , then fit for the amplitude and phase of the polarization sinusoid using a least-squares routine.

The polarimeter offset angle ϕ_{offset} was calibrated by observing the limb of the Moon, which was assumed to be polarized in the radial direction. We found the Moon to have a low fractional polarization of about 1% at 1.3 mm, with a polarization position angle that tracked precisely with rotation angle around the lunar limb (observations were made at radii of $12'$ from the lunar center). From these measurements, plotted in Fig. 2, we found that $\phi_{\text{offset}} = 80.5^\circ \pm 0.7^\circ$ for the setup employed at the 12 m telescope. Figure 3 shows the data for a typical observation of the moon, folded to ten polarimeter-angle bins. The solid line in Fig. 3 is a least-squares fit to the 4θ polarization sinusoid (only one period remains after folding).

Venus was used to calibrate the *fractional* instrumental polarization. Upper limits of $\approx 0.3\%$ were obtained for both

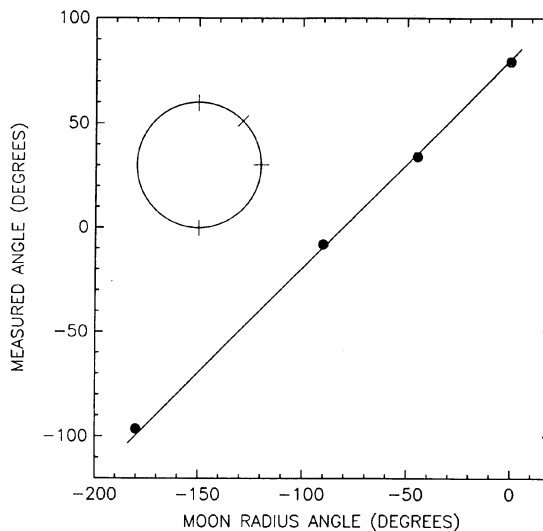


FIG. 2. Measured polarization angle versus Moon radius angle, used to derive the polarization offset angle ϕ_{offset} . The telescope-pointing positions, at radii of $12'$ from the lunar center, and assumed (radial) polarization position angles are indicated by the tick marks on the circle. The fitted line, constrained to have a slope of unity, has an intercept of $80.5^\circ \pm 0.7^\circ$ ($= \phi_{\text{offset}}$).

the fractional instrumental polarization and the fractional polarization of Venus from two sets of observations at parallactic angles differing by 67° . (An advantageous feature of altazimuth telescopes with regard to polarization measurements is that the source, as it crosses the sky, appears to rotate with respect to the telescope; this rotation is described by the change in parallactic angle, and can be used to separate the source polarization, which rotates with parallactic angle, from any instrumental polarization, which is assumed

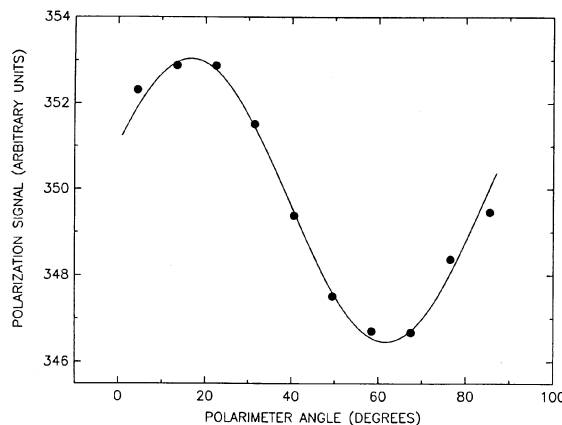


FIG. 3. Typical polarization data for the lunar calibration observations (this example is for Moon radius angle -45°). The original 40 polarimeter-angle bins have been folded to 10, covering one full period of the 4θ polarization sinusoid. The solid line is the fit to Eq. (1) in the text, with $T_p = 6.58 \pm 0.28$ (arbitrary units) and $\phi = 33.5^\circ \pm 1.2^\circ$. The total intensity is twice the mean level of the data, or equivalently, the sum of the minimum level ($=$ (unpolarized intensity)/2) and the maximum level ($=$ (unpolarized intensity)/2 + polarized intensity). The fractional polarization is $0.94\% \pm 0.04\%$ for this measurement.

to be constant. The procedure for extracting source and instrumental components is discussed in the next subsection.) The low limit on the fractional instrumental polarization found using Venus is supported by the lunar observations—any instrumental term at the 0.2% level or greater would have corrupted the position-angle measurements and skewed the data points off the straight line in Fig. 2. Another form of instrumental polarization, at a low absolute level and apparently not proportional to source strength, was found in the observations of Orion.

c) Analysis of the Orion Observations

Two positions, separated by one beamwidth (30") north-south, were observed in Orion (see Table I for coordinates, and Fig. 4 for a 1.3 mm continuum map of the region by Gordon and Jewell (1987)). These positions, designated Orion S(outh) and Orion N(orth), were each observed for about 1 hr both east and west of transit. The observing sequence (with mean parallactic angle in parentheses) was: Orion S(−42°), Orion N(−22°), Orion N(+35°), and Orion S(+48°). Total flux densities, measured using standard continuum beam-switching techniques, are 43.5 ± 5.1 Jy and 83.0 ± 8.8 Jy for Orion S and Orion N, respectively. In the absence of instrumental polarization, or if the instrumental term can be calibrated (using, for example, a planet), measurements of a given source position at various parallactic angles should produce identical results once the known parallactic-angle correction is applied. This was not found to be the case for the Orion measurements, which, for both positions, gave significantly different answers east and west of the meridian (the derived position angles were different by $\approx 30^\circ$). This cannot be explained as being due to an unaccounted fractional instrumental component, because the Venus and Moon measurements show that this component must be less than 0.3%, much too small to significantly affect the several percent polarizations measured.

While the polarization phase did rotate with parallactic angle for Orion, it did not rotate quite enough. It appears that the measurements were corrupted by a source of instrumental polarization unrelated to the astronomical source being observed. If this instrumental effect is constant, it can be separated from the true source polarization because observa-

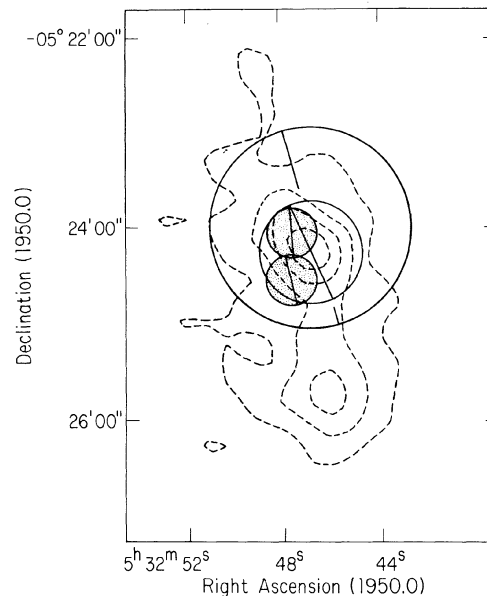


FIG. 4. Comparison of beams and polarization position angles for the three experiments listed in Table II, superposed on a map of the 1.3 mm continuum emission in Orion (from Gordon and Jewell 1987). For clarity, only alternate contours on the map have been retained. The circles, in order of descending size, represent the beams used in the experiments of Cudlip *et al.* (1982), HDN and Dragovan (1986), and this experiment (stippled).

tions are available at two different parallactic angles. By comparing the instrumental polarizations derived below from the Orion S and Orion N data, we find that the instrumental term does indeed appear to be constant in amplitude and phase. However, this term is constant in absolute amplitude (in milliKelvins, or Janskys), rather than being a constant fraction of the source total flux density. It is too weak to have been detected, if present, in the calibration observations of the Moon and Venus.

TABLE I. Summary of Orion measurements.

	Orion S	Orion N	Comments
$\alpha(1950)$	$05^{\text{h}}32^{\text{m}}47.6^{\text{s}}$	$05^{\text{h}}32^{\text{m}}47.6^{\text{s}}$	
$\delta(1950)$	$-05^{\circ}24'33''$	$-05^{\circ}24'03''$	
S_T (Jy)	43.5 ± 5.1	83.0 ± 8.8	Total flux density
T_I (mK) ...	15.3 ± 4.0	19.0 ± 5.1	Instrumental polarization term
S_I (Jy)	1.49 ± 0.39	1.85 ± 0.50	Flux density equivalent of T_I
ϕ_I (degrees)	167.2 ± 7.5	176.6 ± 7.7	Instrumental phase
S_P (Jy)	2.13 ± 0.47	1.52 ± 0.61	Source polarized flux density
P (%)	4.89 ± 1.09	1.84 ± 0.74	Source fractional polarization
χ (degrees)	14.3 ± 6.3	5.2 ± 11.5	Source polarization position angle

d) Instrumental Term Correction

We now describe the procedure for deriving the source and instrumental terms from observations at two different parallactic angles, which is based on the method used by Dragovan (1986). We start with the working hypothesis that the instrumental term is constant. If this is the case, then differencing observations of a source taken at different parallactic angles will cancel the instrumental term, while producing a sinusoid in the data which is the difference between the source polarization sinusoids (which have equal amplitudes but different phases). The result has the form

$$T_{\text{diff}}(\theta, \phi_1, \phi_2) = T(\theta, \phi_1) - T(\theta, \phi_2), \quad (3)$$

where T and ϕ are defined in Eqs. (1) and (2) (the observations are made at parallactic angles η_1 and η_2). Substituting and combining terms yields

$$\begin{aligned} T_{\text{diff}}(\theta, \phi_1, \phi_2) = & T_p \sin[\eta_2 - \eta_1] \\ & \times \cos[4\theta - 2(\chi - \phi_{\text{offset}}) \\ & + (\eta_1 + \eta_2) - \pi/2]. \end{aligned} \quad (4)$$

This is a sinusoid with amplitude $T_p \sin[\eta_2 - \eta_1]$, and a phase term that can be solved to obtain χ , the true source position angle. When $\eta_2 - \eta_1 = 90^\circ$ (as is the case for the Orion S data), the sinusoidal amplitude of the differenced scan is twice the amplitude of the original scans. Similarly, by summing scans it is possible to derive the instrumental polarization, correcting for the source polarization (if necessary) after deriving it as above. The expressions are somewhat complicated, though straightforward, and are not given here. For the special case of Orion S, the source polarization sinusoids are $180^\circ (= 2[\eta_2 - \eta_1])$ out of phase, and add destructively, leaving only the instrumental polarization.

Applying this procedure to the Orion S and Orion N data separately, we find the instrumental and source polarizations listed in rows 4–9 of Table I (quoted errors are statistical only; fractional polarizations are not corrected for noise bias (see, for example, Killeen, Bicknell, and Ekers 1986)). Note that the instrumental polarization has the same phase (to within the errors) for Orion S and Orion N, as well as having the same amplitude when the amplitude is expressed in absolute units rather than as a fraction of the total flux density of the source. The instrumental polarization is significant: for Orion N it is as large as the polarization of the source, and for Orion S it is nearly as large. However, the fact that it is the same for both Orion positions supports the assumption that it is constant with time, so that meaningful values of the source polarization can be derived using the above procedure. Future runs with MILLIPOL should uncover the nature and origin of this instrumental polarization term.

III. DISCUSSION

In order to facilitate comparison of our Orion results with the previous far-IR and submillimeter measurements, which were made with larger beam sizes, we have combined the Orion S and Orion N polarizations. The result is $P_{\text{sum}} = 2.85 \pm 0.61\%$ at $\chi_{\text{sum}} = 10.5^\circ \pm 6.1^\circ$. A comparison of our positions and beam sizes with those of Dragovan (1986) and Cudlip *et al.* (1982) can be seen in Fig. 5. A comparison of the polarizations (summarized in Table II) reveals that the three experiments found very similar polarizations, per-

haps surprisingly so considering the differences in wavelength and beam size. It is likely that the magnetic fields in the Orion KL region are fairly uniform in direction, based upon the similarity of position angles found in the different experiments and in the two positions measured in this experiment. If the far-IR, submillimeter, and 1.3 mm polarizations are due to optically thin emission by spinning grains aligned by magnetic fields, then the position angle of polarization should be perpendicular to the projection of the magnetic field on the sky (Purcell 1979; Davis and Greenstein 1951). Thus our measurements imply a position angle for the magnetic field of 101° .

Optical and near-IR polarizations, caused by selective absorption by spinning grains, will have position angles parallel to the projection of the field on the sky. The interstellar magnetic field in the general area of the Orion Nebula, as determined by polarized starlight, is oriented at $\approx 100^\circ$ (Breger 1976), parallel to the magnetic field implied by our observations. The mid-IR polarization at KL, due to selective absorption of the radiation from embedded sources by aligned grains, has position angles averaging 103° at $11 \mu\text{m}$ and 118° at $20 \mu\text{m}$ (from HDN, who used data of Knacke and Capps 1979), very nearly orthogonal to the 1.3 mm position angle and again indicating fields with nearly the same direction as those measured at 1.3 mm.

A conspicuous structural feature in the Orion Molecular Cloud is the large scale ($\approx 10' \times 30'$) Orion Ridge feature seen in the IR continuum and in many molecular species (e.g., Kutner *et al.* 1976; Smith *et al.* 1979). Its orientation at a position angle of about 10° is aligned with our measured 1.3 mm polarization position angle, and is thus perpendicular to the magnetic field direction implied by our measurements and the others noted above. The Orion Ridge may have formed as material collapsed along the field lines, having been prevented by magnetic forces from collapsing across the field lines. One final comparison of angles is worth noting: the axis of the high-velocity bipolar outflow at KL (e.g., Wright *et al.* 1983) is approximately along the direction of the magnetic field in Orion as derived from the polarization data.

It is beyond the scope of the present work to consider the possible implications of 1.3 mm polarimetry for understanding the properties of grains (see Dragovan (1986) for a discussion of grain properties and submillimeter polarization). It will be of interest to fully sample, at 1.3 mm, the beam areas observed by HDN and Dragovan (1986) at $270 \mu\text{m}$, so that a direct comparison can be made of the polarizations at the two wavelengths. Different types of grains (graphite, silicates) have different magnetic properties and should exhibit different degrees of alignment in magnetic fields. By comparing the fractional polarizations it may be possible to constrain models for the relative emissivities as a function of wavelength for graphite and silicate grains (Dall'Oglio *et al.* 1976; Hildebrand 1984).

Our primary objective in these initial observations with MILLIPOL was to demonstrate the viability of the instrument and the feasibility of ground-based short millimeter-wavelength polarimetry as applied to emission from dust. Our measurements of significant polarization in Orion, though preliminary, indicate that fruitful mapping of magnetic fields in molecular clouds will be possible at the relatively high angular resolutions available with large ground-based millimeter and submillimeter telescopes. We plan to continue this work at 1.3 mm by mapping a larger area in

TABLE II. Comparison of Orion polarization measurements.

	λ	Beam Area	P	χ
	(μm)	(arcmin^2)	(%)	(degrees)
Cudlip <i>et al.</i> (1982)	77	3.1	2.2 ± 0.4	16 ± 8
Dragovan (1986)	270	0.8	1.7 ± 0.2	24 ± 6
This paper (combined result)	1300	0.4	2.9 ± 0.6	11 ± 6

Orion and surveying other molecular cloud regions with strong dust emission, and we hope to eventually move to shorter wavelengths, where the flux densities are much larger due to the steeply rising spectrum of grain emission.

This research has been supported in part by a Cottrell Research Grant from the Research Corporation to D.C. We wish to thank the NRAO Tucson staff for mounting MILLIPOL in their receiver system and providing technical and

moral support for the MILLIPOL experiment. We also wish to thank the NRAO Central Development Lab, and especially Peter Siegal, for assistance in testing the polarization analyzer, and Raoul Erickson for assistance with the electronics. The A/D board was loaned from the Steward Observatory Mirror Oven Project. R.B. thanks Neil Killeen and Stefi Baum for useful (to him) and at times maddening (to them) discussions of polarimetry. Finally, we extend our appreciation to Mark Gordon and Phil Jewell for allowing us to use their map of Orion in advance of publication.

REFERENCES

- Barvainis, R., and Predmore, C. R. (1984). *Astrophys. J.* **282**, 402.
 Barvainis, R., and Wootten, A. (1986). *Astron. J.* **92**, 168.
 Breger, M. (1976). *Astrophys. J.* **204**, 789.
 Cudlip, W., Furniss, I., King, K. J., and Jennings, R. E. (1982). *Mon. Not. R. Astron. Soc.* **200**, 1169.
 Dall'Oglio, G., *et al.* (1976). In *Planets, Stars, and Nebulae Studied with Photopolarimetry* (University of Arizona, Tucson), p. 336.
 Dragovan, M. (1986). *Astrophys. J.* **308**, 270.
 Goldreich, P., and Kylafis, N. D. (1981). *Astrophys. J. Lett.* **243**, L75.
 Gordon, M. A., and Jewell, P. R. (1987). Preprint.
 Hildebrand, R. H., Dragovan, M., and Novak, G. (1984). *Astrophys. J. Lett.* **284**, L51 (HDN).
 Hildebrand, R. H. (1983). *Q. J. R. Astron. Soc.* **24**, 267.
 Killeen, N. E. B., Bicknell, G. V., and Elkers, R. D. (1986). *Astrophys. J.* **302**, 306.
 Knacke, R. F., and Capps, R. W. (1979). *Astron. J.* **84**, 1705.
 Kutner, M. L., Evans II, N. J., and Tucker, K. D. (1976). *Astrophys. J.* **209**, 452.
 Purcell, E. M. (1979). *Astrophys. J.* **231**, 417.
 Sutton, E. C., Blake, G. A., Masson, C. R., and Phillips, T. G. (1984). *Astrophys. J. Lett.* **283**, L41.
 Wannier, P. G., Scoville, N. Z., and Barvainis, R. (1983). *Astrophys. J.* **267**, 126.
 Wright, M. C. H., Plambeck, R. L., Vogel, S. N., Ho, P. T. P., and Welch, W. J. (1983). *Astrophys. J. Lett.* **267**, L41.